Proceedings of
11th European Conference on Turbomachinery Fluid dynamics & Thermodynamics
ETC11, March 23-27, 2015, Madrid, Spain

DESIGN OF AN ENGINE QUICKSTART SYSTEM FOR ROTORCRAFT APPLICATION

M. Kerler, C. Schäffer, W. Erhard

Institute for Flight Propulsion, Technische Universität München
Boltzmannstr. 15, 85748 Garching, Germany
martin.kerler@tum.de

ABSTRACT

Current helicopters of the light and medium class have two engines installed due to safety reasons. However, this installed power is rarely needed during a flight mission and the engines are operating mainly in part load leading to poor specific fuel consumption. An intended shutdown of one engine during flight increases the load of the remaining engine and the overall fuel consumption gets better. In case of a failure of the remaining running engine, the shut-off engine has to be quick-start capable due to flight safety reasons.

Therefore, a quick-start system for the Allison 250-C20B engine was developed at the Institute for Flight Propulsion. This system drives during engine start-up the radial compressor of the engine using pressurized air. Since shop air is actually used for the quick-start system, a new system is designed for independent air supply and for integration into a helicopter airframe. It comprises of pipes, hoses, valves and pressure tanks. This new pressurized air supply is simulated in ESPSS. For identification of the usability of ESPSS a validation is done. For this validation the shop air supply system is modeled in ESPSS and a quick-start is simulated. Simulation results of this model are compared to experimental data of the test bed.

NOMENCLATURE

Abbreviations

CAD	Computer Aided Design
CASS	Compact Air Supply System
DDAS	Dynamic Data Acquisition System
ESPSS	European Space Propulsion System Simulation
FADEC	Full Authority Digital Engine Control
GG	Gas Generator
HPC	High Pressure Compressor
HPT	High Pressure Turbine
LPT	Low Pressure Turbine
QSS	Quick-Start System
SASS	Shop Air Supply System
SFC	Specific Fuel Consumption
TOT	Turbine Outlet Temperature
MTOW	Maximum Take-Off Weight

Symbols

d	difference	[-]
K_V	Flow Factor	[m³/h]
$\dot{m}$	Mass Flow	[kg/s]
p	Pressure absolute	[Bar(a), Bar(g)]
T	Temperature	[°C, K]
$\dot{V}$	Volume Flow	[m³/s]

Subscripts

A	Exit
calc	Calculated Value
d	Nozzle
E	Entry
s	Static
t	Total

INTRODUCTION

The current helicopter power train design of light and medium class helicopters is mainly driven by safety reasons. Thus, these helicopters have two or more engines installed. However, up to 60% of the helicopter flight mission time the available installed maximum continuous power of the engines is not needed (Paramour and Sapsard, 1981). Hence, the engines are running most of their operation time in

part load. But turboshaft engines have their lowest specific fuel consumption (SFC) at high engine loads. An operational strategy can be an intended shutdown of one engine during a flight mission. At the same time, the load of the remaining running engine is increasing and the overall SFC is shifted to better values resulting in fuel saving.

Since two or more engines are installed due to safety reasons, an intended shutdown of one engine due to fuel saving during flight mission would reduce the flight safety since there is no power available anymore if the remaining running engine has an engine failure. A possible solution to overcome this problem would be an engine start of the before controlled shut down engine during this emergency situation and using the regained power to perform a secure landing. Nevertheless, a regular engine start from off to idle is up to 26 seconds and from idle to full power up to 4 seconds. During autorotation helicopters are losing 8 to 15 meters of height per second. Thus, in worst case the helicopter encounters a total height loss of about 450 meters until sufficient engine power is available again (Hönle et al., 2012).

An approach to minimize the height loss is reducing the start time of turboshaft engines. At the Institute for Flight Propulsion a quick-start system (QSS) for the Allison 250-C20B engine was developed. The casing of the radial compressor is equipped with five impingement nozzles which are well positioned to provide highest core engine rotor acceleration. The nozzles are provided with air for approximately 2.2 seconds with a total pressure of 12.3 Bar(a) and with an overall mass flow of 0.5 kg/s (Hönle, 2014). Thus, the engine reaches idle within 2.4 seconds from off state (see Fig. 1) and delivers reliably 60 kW (= 20% of max. continuous shaft power) of shaft power within approximately 8 seconds after initiating the quick-start (see Fig. 2). For power delivery tests the dynamometer at the testbed is preset at 100 Nm brake torque.

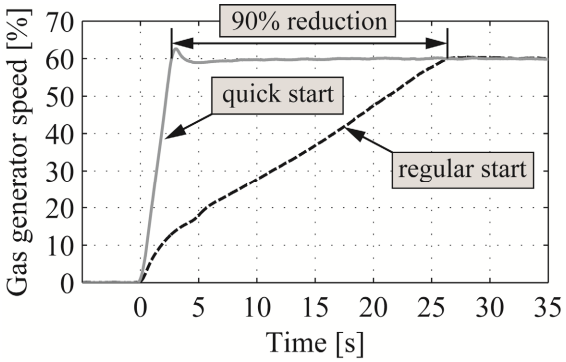

Fig. 1: **Ground idle start times of a regular engine start and a quick-start**

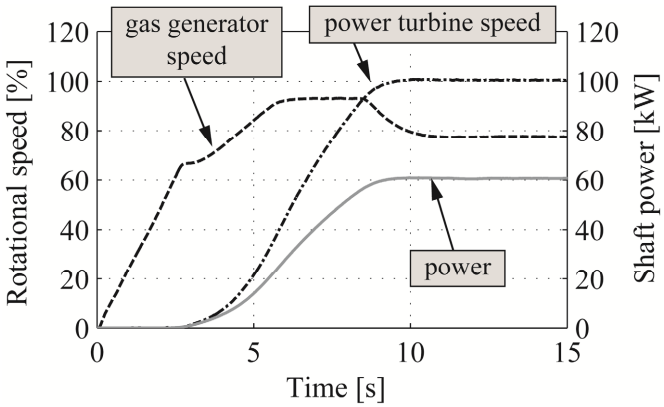

Fig. 2: **Power delivery curve after performing a quick-start to flight mode**

However, this QSS is supplied by shop air and thus, not capable of being integrated into a helicopter. Hence, a system has to be developed which provides sufficient pressurized air for the nozzles. Furthermore, the QSS must be of compact dimension for helicopter airframe integration without any extensive structural airframe modifications. For this purpose, the software ESPSS (ESPSS, 2014) is used for rapid modeling and simulation of several possible design concepts of the compact air supply system (CASS). ESPSS is usually used for simulation of space propulsion systems and has a component library which offers appropriate objects for modeling the CASS. ESPSS utilizes the framework provided by the generic system simulation tool EcosimPro which is a state-of-the-art tool for modelling of dynamic systems represented by differential-algebraic equations as well as ordinary differential equations and discrete events (Isselhorst, 2010; Pérez-Vara et. al., 2003; Moral et. al., 2010).

For simulation tool validation the current QSS with shop air supply system (SASS) is modelled with ESPSS and simulated. The results are compared to experimental data of a quick-start and possible deviations are identified. Then, with given requirements one preliminary CASS is designed, modelled and simulated. Based on these results the preliminary design variant is evaluated and advice for further proceeding is given.

ENGINE, TEST BED AND EXPERIMENTAL SETUP

The experimental investigations of the presented turboshaft engine QSS are carried out on an Allison 250-C20B turboshaft engine of the Institute for Flight Propulsion at Technische Universität München. This turboshaft engine has several applications such as helicopter and turboprop drive. The engine installed at the test bed powered formerly an Airbus Helicopters BO 105 helicopter of German Armed Forces. Its maximum continuous power is approximately 300 kW. Despite the engine design from the late 1960's modified versions of the Allison engine are still in production at Rolls-Royce North America.

The engine has two spools and its modular design enables an easy exchange of engine parts. The high pressure compressor (HPC) is of axial-radial design and comprises a six stage axial compressor and a final radial compressor stage. The single reverse-flow combustion chamber is fed by two ducts with the compressor mass flow. A two stage axial high pressure turbine (HPT) drives the HPC and via a gearbox the auxiliaries such as oil pump, fuel pump or starter generator. The HPT is followed by a two stage axial low pressure turbine (LPT) which provides via the low pressure shaft and a reduction gearbox the useable shaft power.

For several research activities the engine is equipped with additional sensors compared to the normal operation instrumentation. Areas of low temperature such as compressor inlet, bleed air valve, exhaust as well as fuel are measured using Pt100 sensors. Areas of high temperature such as the one between the HPT and LPT are covered by NiCr-Ni typ K thermocouples. For recording the ambient pressure, a gauge pressure sensor was used. Other pressure metering points were realized with differential pressure sensors which are listed in Table 1 (Kerler et. al., 2013). The positions of the measuring points can be seen in Fig. 3.

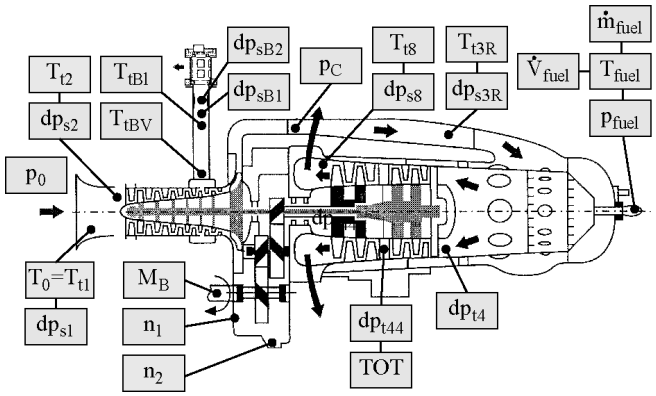

Fig. 3: **Instrumentation of the test bed engine**

The torque of the output shaft is recorded using the engine's internal torque metering device as well as using a strain gauge between dynamometer basement and dynamometer's wheel casing. Air mass flow of engine's inlet and bleed air section are determined via Venturi tubes. Fuel flow is measured by a turbine flow meter for dynamic measurements and by a scale for static measurements.

Table 1: **Pressure sensors of the test bed engine's instrumentation**

Sensor Manufacturer and Typ	Range	Position
Setra Systems, Model 280	0 to 1.7 Bar(g)	dp_{t44}
Setra Systems, Model 280	0 to 6.9 Bar(g)	dp_{t4}
Setra Systems, Model 280E	0 to 6.9 Bar(g)	dp_{s3L}, dp_{s3R}, dp_{t4}
Setra Systems, Model 239	0 to +/- 38 mBar(g)	dp_{s8L}, dp_{s8R}
Setra Systems, Model 239	0 to 127 mBar(g)	dp_{s2}, dp_{sb1}, dp_{sb2}
Setra Systems, Model D239	0 to 25 mBar(g)	dp_{s1}

In addition, the original compressor pressure controlled bleed air valve was replaced by a remote controlled bleed air valve to extend engine control possibilities. Furthermore, the original installed hydro-mechanical fuel flow governor does not allow any practical manipulation of the metered fuel flow. Thus, it was replaced by an own developed fuel flow controller based on the design principles of

modern FADEC systems and a related electro-mechanical valve control unit for the actual fuel metering. Further information is provided in (Gabler, 1998) and (Kerler et. al., 2013). Besides a data acquisition system for continuous data recording at 2 Hz, a dynamic data acquisition system (DDAS) is available. It is capable of recording all channels with a sampling rate of 1 kHz.

QUICK-START SYSTEM

The acceleration of the engine's high pressure components such as HPC and HPT is based on the impingement of the radial compressor blades with a high speed air jet. A short description is given in the next section. Further details can be found in (Hönle, 2014). Then, the relevant experimental setup is described for validation purposes of the system's ESPSS model.

System description

As there are several possibilities for acceleration of the high pressure components (Hull et. al., 1967) an evaluation was carried out for identifying the best solution. It revealed that impingement Laval nozzles at the end of the radial compressor's impeller are the best solution to meet performance and cost requirements. Thus, an integration of Laval nozzles within the radial compressor casing was investigated. Based on system performance calculations and available installation space at the compressor casing the number of Laval nozzles was defined as 5. The nozzles have a minimum inner diameter of 6.6 mm and are asymmetrically positioned at a certain angle to provide best acceleration of the gas generator (Hönle et. al., 2012; Hönle, 2014). The main parameters of the QSS are given in Table 2 and a CAD image of the compressor with the engine related QSS components is given in Fig. 4.

Table 2: **Parameters of the QSS**

Parameter	Value	Parameter	Value
Total mass flow:	0.5 kg/s	Minimum nozzle diameter:	6.6 mm
Air velocity at nozzle exit:	Mach 2.3	System active time:	2.2 s
Total pressure at nozzle entry:	12.3 Bar(a)	System deactivation limit:	58% GG spool speed

The five nozzles are supplied by shop air which has a supply pressure of approx. 13 Bar(a) and a maximum mass flow rate of 3 kg/s. Since the total mean mass flow of the QSS is 0.5 kg/s, the mass flow through one nozzle is 0.1 kg/s. Due to the integration of the nozzles within a new radial compressor casing, the inner surface of the casing is not completely plain anymore but has five elliptic holes. Accordingly, the nozzle outlet cross section is therewith tapered and also elliptic. Several engine tests were conducted to determine the influence of these holes on overall engine performance. As a result, the compressor has an isentropic efficiency loss of less than 1% for all mass flows above ground idle speed and the pressure ratio is not influenced in an unacceptable manner (Hönle et. al., 2012).

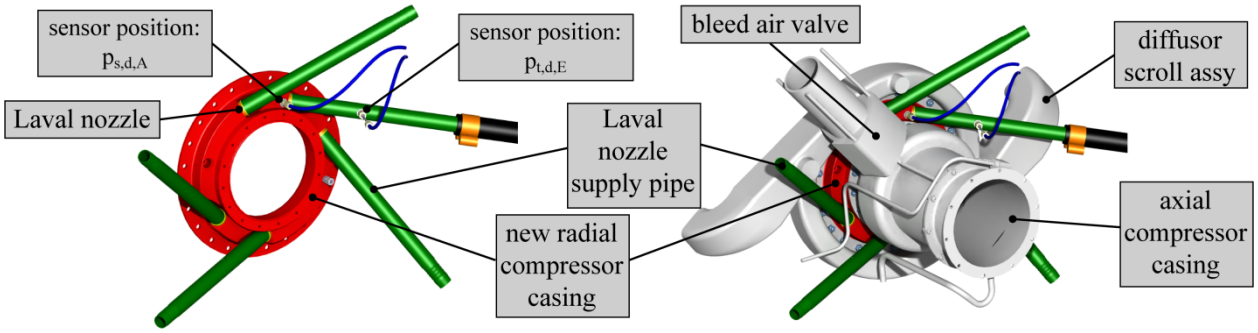

Fig. 4: **Integration of the new radial compressor casing with 5 supply pipes**

The SASS is designed as the diagram in Fig. 5 shows as follows. It operates with two pressure systems. The approx. 13 Bar(a) shop air is used for the Laval nozzles whereas the 8 Bar(a) shop air is used for operation of the pneumatic piston 2/2-way valve by a remote controlled 3/2-way solenoid valve. The manifold block splits the 13 Bar(a) shop air supply into five equal feeds for the Laval nozzles. An additional manually operated ball valve is located just before the 2/2-way valve due to

safety reasons. After engine tests with quick-start and after closing the main cut-off cock, the SASS is ventilated with the vent cock.

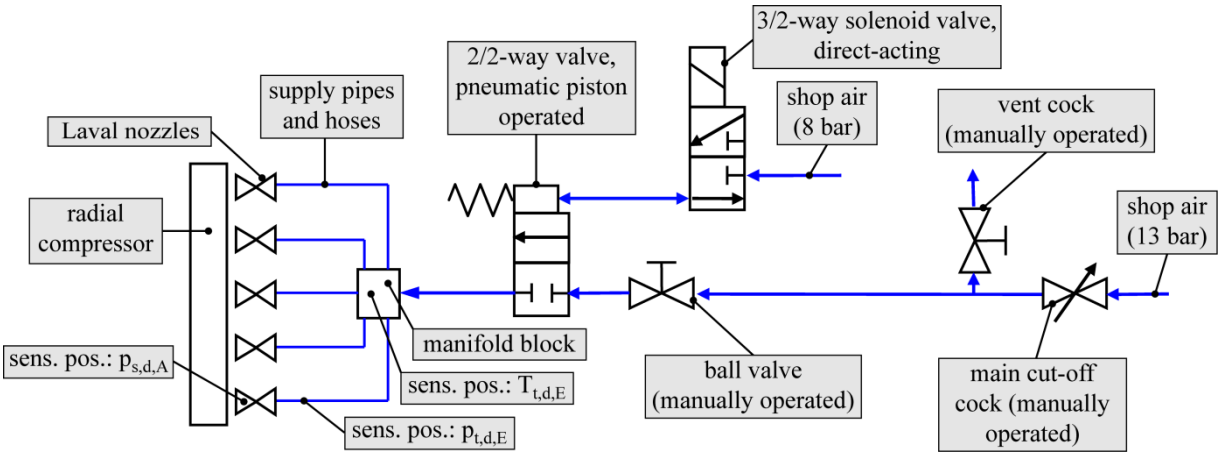

Fig. 5: **Functional overview of the SASS with three additional sensor positions**

Additional experimental setup

Besides the regular used engine instrumentation additional instrumentation, was installed for the SASS. These three new sensor positions can be seen in Fig. 5 and are connected to the DDAS with a sampling rate of 1 kHz. Furthermore, an own compressor test rig was designed for first acceleration tests prior to engine tests. At this test rig, the static pressure measuring point is at the smallest diameter of the elliptic outlet cross section of the Laval nozzles. This measuring position has been changed for the Laval nozzles of the built-in new radial compressor casing. The position moves a few millimeters upstream towards a smaller nozzle diameter. The reason for this was getting more data regarding the nozzle flow. Determination of the total pressure just before the nozzle entry is realized by a pitot tube inside the supply pipes. The total pressure and static pressure measuring points are connected via a 5 m hose to the pressure transducers. Information about the pressure transducers is given in Table 3. Since research on the QSS is funded only by the Institute and financial possibilities are limited, already available pressure transducers were chosen. The total temperature of the pressurized shop air just before the nozzles is measured inside the manifold block (see Fig. 5). For initial operation tests of the QSS a gap sensor was installed at the radial compressor to determine the axial clearance variation during quick-starts for detecting possible rubbing. As a result, the clearance between impeller and casing is not critical in any case (Hönle, 2014). For extensive validation purposes of the ESPSS model of the QSS with SASS, more sensor locations are preferable. However, back then a validation of a simulation model was not planed and the instrumentation was sufficient for performing the initial operation of the QSS in an empirical manner (Hönle et. al., 2012; Hönle, 2014).

Table 3: **Additional pressure sensors of the SASS**

Sensor Manufacturer, Sensor Model	Range	Position	Response Time	Frequency Solution
Walcher, Model SDX15D-A	0 to +/-1 Bar(g)	$p_{s,d,A}$	< 100 µs	1000 Hz
Parker, Model SCPSD-016-04-17	-1 to 16 Bar(g)	$p_{t,d,E}$	< 10 ms	200 Hz

Comparison of experimental data with the simulation model

The ESPSS simulation model of the QSS is modelled in a way to meet the real system parameters as much as possible with justifiable simplifications. Thus, model elements are defined with given data of the QSS components. If no data was available, parameters were measured for instance. The friction of the Laval nozzle walls are neglected as well as the manifold is set adiabatic. ESPSS requires the smallest diameter of a valve as input parameter. Based on technical drawings the smallest diameter of the 2/2-way valve is identified as 25 mm since the valve's data sheet provides no detailed information. On the other hand, the guaranteed valve's flow factor K_V is $37\ m^3/h$ and therewith higher than the calculated one ($K_{V,calc} = 15\ m^3/h$) for the present system. Thus, the smallest diameter of the valve shouldn't have any influence on the system's performance. Unfortunately, opening and closing times of

the 2/2-way valve are not given in the valve's documentation. Thus, based on similar valves the opening and closing time is defined as 360 ms. The operating time of the QSS and therewith the 2/2-way valve is set to 2.2 s since the gas generator spool speed reaches after 2.2 seconds from off-state 58%. At 58% the FADEC deactivates the QSS and therewith closing of the 2/2-way valve is initiated. The compressed shop air is produced by a screw compressor. The required compressed air volume for a quick-start is approx. 75 dm³. Since this volume is stored in the shop air pipes and hoses of the SASS for a longer time, it can be assumed the shop air has a temperature close to room temperature of about 20 °C. Thus, the shop air temperature of the ESPSS model ist set to 293.15 K which equals 20 °C. The shop air pressure is set to 12.75 Bar(a) which is an average value since the shop air pressure has a certain tolerance range caused by the shop air system. The created ESPSS model of the QSS with SASS looks as follows (see Fig. 6).

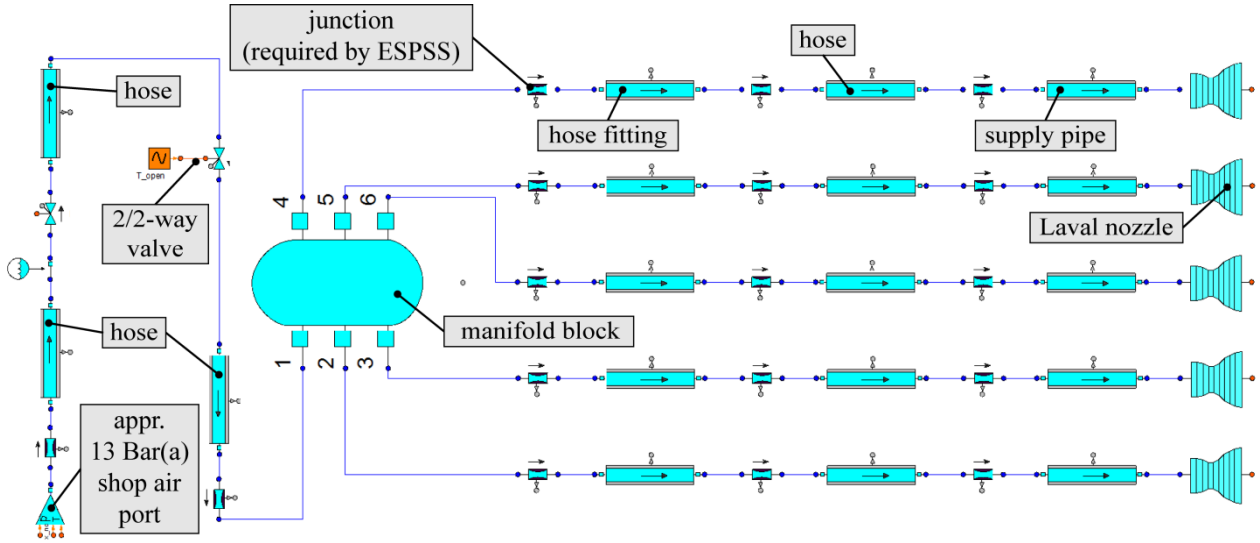

Fig. 6: **ESPSS model of the QSS with SASS**

Since ESPSS allows the selection of air as ideal gas or as real gas a short evaluation of the differences is made. For this, values of total pressure, static pressure and Mach number after the nozzle are compared. As a result the deviation of ideal gas to real gas is less than 2% for the relevant time range. However, all further calculations are performed with setting real gas.

The first evaluation of the model regarding experimental data is related to the total pressure inside the supply pipes short before the nozzles. At first glance both simulation and experiment show a similar behavior of the evolving total pressure (see Fig. 7). In particular, the maximum total pressure fits well and has only a maximum deviation of 1% at time step 3 seconds. However, the pressure increase gradient of the measured values is a bit slower than the simulated one. This may be due to the dynamic response of the sensor chain.

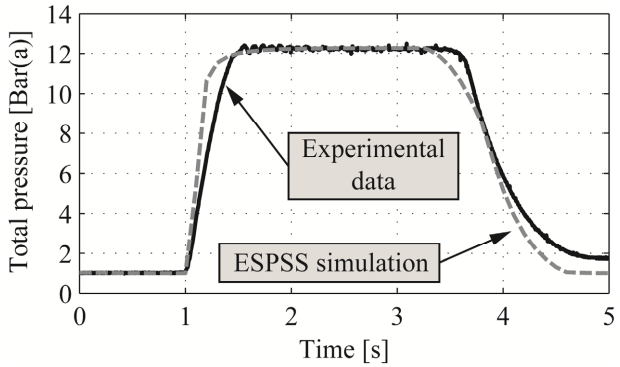

Fig. 7: **Total pressure short before Laval nozzle entry**

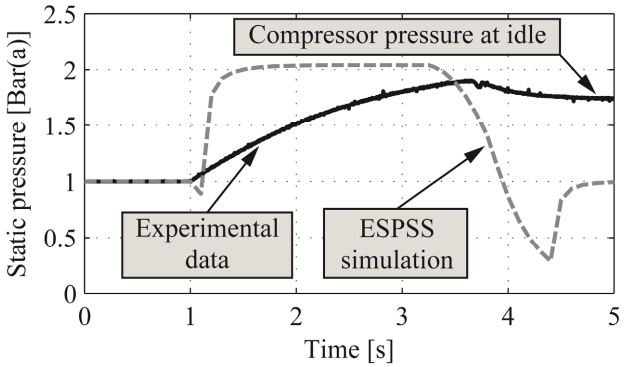

Fig. 8: **Static pressure short after smallest diameter of the Laval nozzle**

The curves of the measured and simulated static pressure show a totally different behavior. The measured static pressure is only slowly increasing. Performing an extrapolation of the measured static pressure curve after time step 3.8 seconds reveals a leveling at approximately 2.05 Bar(a). This value is also reached by the simulation but after a very short time of 0.7 seconds. An explanation of this may be the very complex flow field inside and after the nozzle. The nozzle's outlet is slanted and during engine start-up the blades of the radial compressor are passing by, causing some kind of time varying part blockage. Thus, boundary layer separation inside the nozzle may happen, causing reverse flow areas with ambient pressure. Thus, not just the static wall pressure of a fully developed nozzle flow field is measured, but rather some kind of compressor pressure at the trailing edge of the radial compressor rotor. Schlieren tests were performed with a fixed radial compressor trailing edge rotor dummy to simulate the part blockage of the blade passages (see Fig. 9). The following Figure 9 shows a shock, its reflection and some expansion waves. However, lowering the Laval nozzle inlet total pressure the shock is moving upstream into the nozzle. Thus, moving blades may have some similar effects and leading after all to the measured static pressure at the wall static pressure bore.

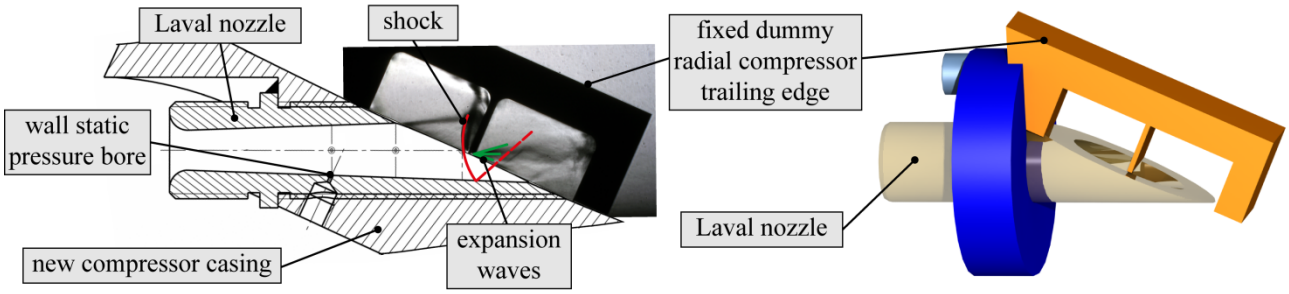

Fig. 9: **Schlieren image of the nozzle outlet with blade passage blockage at Laval nozzle inlet total pressure of 12.6 Bar(a)**

Unfortunately, the ESPSS model does not allow the simulation of a time varying ambient pressure at the nozzle outlet. Because of this, the model has as boundary condition a fixed ambient pressure of 1 Bar(a) at the nozzle outlet. The experimental data was recorded during a real engine quick-start. Thus, the static pressure as well as the total pressure is leveling to the pressure at the impeller trailing edge. This pressure is approx. 1.7 Bar(a) for engine idle speed and can be clearly observed at time step 5 seconds of Fig. 7 and Fig. 8.

A further available measured parameter for evaluation purposes is the total temperature in the manifold. The recorded experimental data curve can be seen in Fig. 10 as thick black line. After the opening of the 2/2-way valve and getting the Laval nozzles choked the manifold as well as the hoses and pipes are like a closed volume. Because of this, the compression of the air inside the system causes a temperature increase. Due to the slow time response of the thermocouple this increase at time step 1.1 second can hardly observed. However, the simulation shows it. After that, the temperature of the compressed shop air can be observed. Due to thermocouples time behavior the measured temperature is slowly decreasing. When 2/2-way valve closing starts, the remaining volume of compressed air inside the QSS is expanding and therewith its temperature is decreasing until ambient pressure is reached. Again, keeping thermocouples time behavior in mind, the measured data show similar behavior. The ESPSS model delivers only static temperatures inside the manifold. Thus, a reasonable comparison to the total temperatures during the highly dynamic quick-start is not practicable. To overcome the slow thermocouple response times, a dynamic time correction may improve the dynamic behavior and its informative value. However, reliable information about accurate air temperatures inside the manifold is not essential for further preliminary design of CASS.

Determination of the mass flow through the nozzles and the Mach number at the nozzle exit are relevant parameters for future CASS since both parameters have a high influence on the overall system performance and therewith gas turbine acceleration during quick-start. Earlier experimental measurements revealed a nozzle mass flow of 0.1 kg/s +/- 5% which is marked in Fig. 11 as thick black line with upper and lower deviation at 0.105 kg/s and 0.095 kg/s as dotted grey lines. The deviation is mainly caused by pressure oscillation of the shop air. The simulation results are very close to the experimental data. Short before main valve closing the simulated mass flow is of 0.102 kg/s and

therewith it has a deviation of 2% neglecting the pressure oscillation. Thus, the mass flow of the nozzles is predictable with the simulation model.

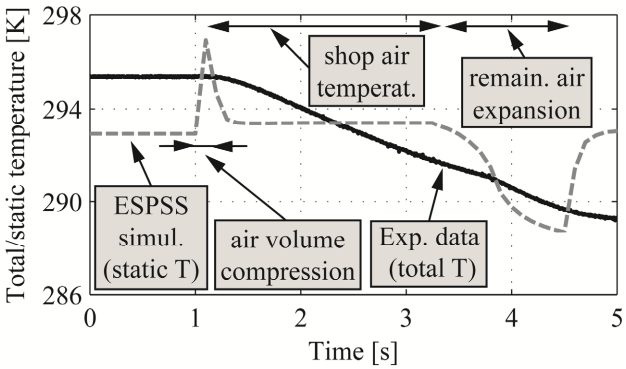

Fig. 10: **Static and total temperature inside the manifold with the SASS**

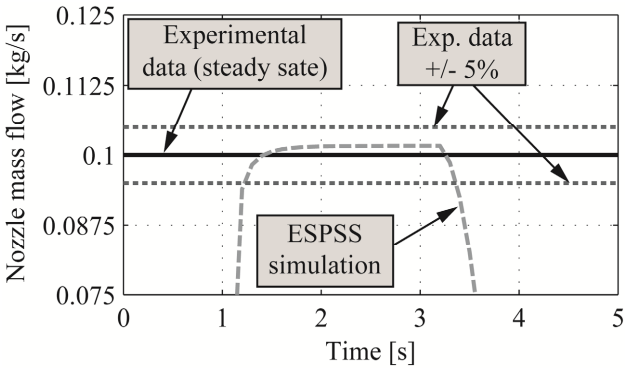

Fig. 11: **Mass flow through one Laval nozzle with the SASS**

Besides the mass flow the Mach number at the Laval nozzle exit is also a matter of particular interest due to determination of the impingement forces. The design Mach number of the Laval nozzle is 2.3 which is marked in Fig. 12. Experimental tests of the Laval nozzle with different entry pressures and the same ambient pressure at the nozzle outlet were performed for validation of analytical and numerical calculations. For this purpose, Schlieren pictures were taken (Barth, 2011). The Schlieren picture visualizes the Mach lines, Mach disks, shock waves as well as expansion waves. The shock wave angel shows a flow velocity of Mach 2.5 (with 12.46 Bar(a) total pressure at nozzle entry) before the shock, which is higher than the design Mach number of the nozzle and marked with a dotted dark grey line in Fig. 12. CFD Calculations (see Fig. 13) show a similar flow pattern and the Mach number at the nozzle exit is 2.57 (thick black line in Fig. 12) (Ullrich, 2011). The final Mach number before valve closing calculated with ESPSS is 2.42 and fits between the values of the design Mach number and the experimental results. However, the engine's built-in Laval nozzles are canted which results in different flow patterns as well as different parameters at the nozzle's canted exit. Furthermore, during engine start-up acceleration the blades of the radial compressor are passing by, causing a highly transient flow pattern hence it is more difficult to determine the Mach number at the nozzle exit. Nevertheless, for preliminary design the ESPSS calculated value is sufficient and reliable.

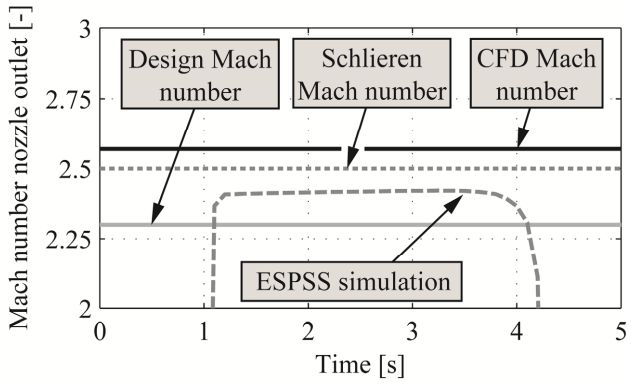

Fig. 12: **Mach number at nozzle outlet with the SASS**

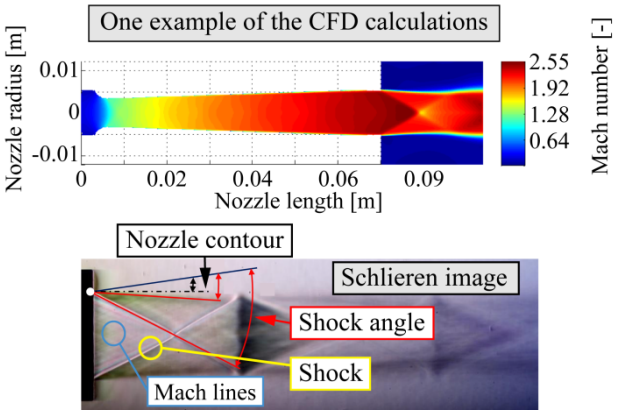

Fig.13: **CFD calculations and Schlieren tests for the nozzle at design point (Ullrich, 2011; Barth, 2011)**

The last parameter of the QSS is the thrust of the Laval nozzles. To determine the nozzle thrust, the compressor of the compressor test rig was locked and with a load cell and lever the torque was measured. Then calculations showed a mean thrust of 51 N for each nozzle during steady state operation. ESPSS is determining the nozzle thrust to 52.1 N shortly before deactivating the QSS as Fig. 14 shows. In summary, Table 4 shows the relevant evaluation parameters.

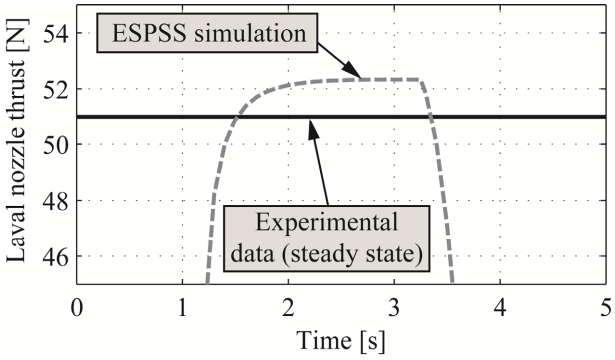

Fig. 14: **Laval nozzle thrust with SASS**

Table 4: **Overview of values and deviations of relevant system parameters**

Parameter	Value ESPSS	Experiment or Calculation	Deviation [%]
Total pressure [Bar(a)]	12.28	12.3	-0.1
Static pressure [Bar(a)]	2.04	1.9	+7.4
Mass flow [kg/s]	0.102	0.1	+2
Mach number [-]	2.42	2.5	-3.2
Nozzle thrust [N]	52.3	51	+2.5

Overall, the simulation tool ESPSS is determined as sufficiently accurate for performing simulations of the following preliminary CASS design and the results can be used for further concept assessment.

PRELIMINARY DESIGN CONCEPT OF A COMPACT AIR SUPPLY SYSTEM

As already mentioned, the CASS should fulfill certain main requirements which are listed in the following section. However, a final design will be a compromise of all requirements since it is usually not always possible to stick strict to them in any way.

Requirements

The probable most challenging requirement is the placing of the CASS inside the helicopter fuselage without changing structural elements as well as the general shape of the helicopter. Since the research is carried out on the Allison engine the rotorcraft Airbus Helicopters BO 105 is used for integration analysis. Therefore, the engine bay was modeled in CATIA V5 and the Allison engine was integrated into the model (Maier, 2014). The result can be seen in Fig. 15 with removed engine cowling. However, some place is still available for further installations (see marked areas in Fig.15) but other constraints like heat emissions from the combustion chamber have to be taken into account. Other limits for CASS installation are pipe installations for fuel and oil as well as compressor air. These pipes and hoses may be replaced for optimization of available space.

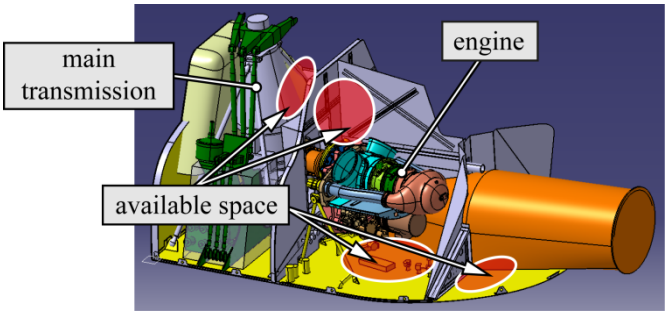

Fig. 15: **CAD model of the BO 105 engine bay for installation space analysis**

Another requirement affects safety issues. Since the QSS is used during an emergency situation its successful operation has to be guaranteed. On the other hand, a malfunction of the system during regular engine and helicopter operation should not have any effect on flight safety. Thus, the system has to be fail-safe. This also applies for ground operations.

To reduce the influence of the CASS due to remaining pressurized air after successful quick-start, one option may be a non-return valve short before the nozzles. Therewith, also the influence of the dead volume of the QSS can be minimized. Beyond that, the QSS should be as simple as possible. Thus, it should have few components and should require little or no maintenance. This comes along with little additional weight to keep its influence on flight performance and payload down.

For the preliminary design a requirement is to keep the nozzle entry total pressure close to 12.3 Bar(a) for the whole QSS operating time since this is the designed operating pressure of the Laval

nozzles and the functionality has been effectually proven. Therewith, the CASS has to provide at any operation time the required mass flow of 0.1 kg/s for each nozzle.

Several design concepts were considered to meet the given requirements. The one most relevant is presented in the following.

Preliminary Design Concept: Single pressure tank per nozzle, five feeds, pyrotechnical valve

The design concept discussed in this paper uses five 300 Bar(a) pressure tanks. Each tank supplies one Laval nozzle with the required mass flow and the corresponding system for one Laval nozzle is illustrated in Fig. 16. The pressurized air is released by a pyrotechnical valve which enables advantageous opening times of less than 7 ms. The length of the connection pipe is defined as 2 m considering installation positions not close to the engine. Further downstream is an orifice for pressure reduction since the total pressure at the nozzle entry should be close to 12.3 Bar(a). For dead volume reduction and prohibiting further streaming out of the pressure tank a close valve is integrated. It closes 2.2 seconds after firing of the pyrotechnical valves. An installation of the close valve short before the nozzles would be the best solution but, because the installation space close to the nozzles at the compressor casing is restricted, there is a hose and a short supply pipe installed between pyrotechnical valve and nozzles. This is also shown in Fig. 16.

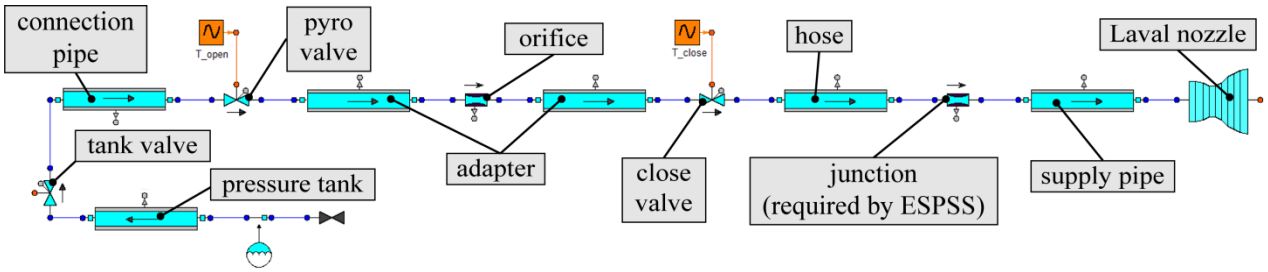

Fig. 16: **ESPSS model of one nozzle of the QSS with CASS**

Further parameters like friction in hoses as well as other effects are defined as in the SASS ESPSS simulation model. The main focus of the preliminary design evaluation lies on the pressure tank pressure during QSS operation, the Mach number at the Laval nozzle outlet, the mass flow through the Laval nozzle and as the most important parameter the Laval nozzle thrust. Fig. 17 shows the static pressure inside the pressure tank. The pressure drop is about 100 Bar(a) what means at the end of the QSS operation air of 209 Bar(a) pressure remains unused in the pressure tank. However, this end pressure is required to maintain a mass flow of 0.1 kg/s during the whole QSS operation time. The simulation result of the flow Mach number at the Laval nozzle exit is as expected (see Fig. 18). It has the same value of 2.42 as the validation simulation in Fig. 12.

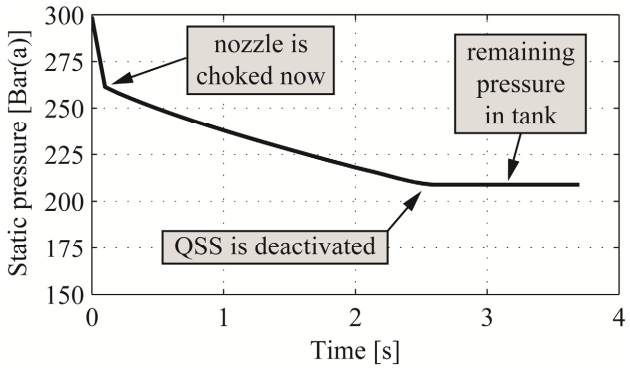

Fig. 17: **Static pressure of the pressure tank**

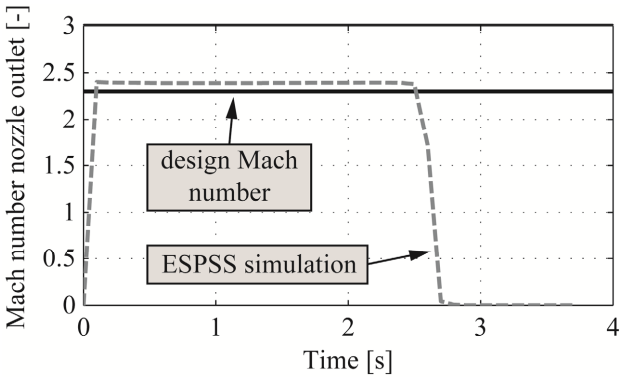

Fig. 18: **Mach number nozzle outlet with the CASS**

As already mentioned, the mass flow and therewith the Laval nozzle thrust should be kept constant for the whole QSS operation time range. This condition is accomplished as Fig. 19 shows. Just before the mass flow falls below the 0.1 kg/s requirement the QSS is deactivated. However, not the whole pressure tank air mass content can be used for the quick-start because a fixed area orifice is used.

Finally, the thrust can be kept mostly above the required 51 Nm. After 2 seconds it drops below this value. Nevertheless, at the beginning of the QSS operation there is a higher thrust of maximum 54.9 N which compensates the small thrust drop after 2 seconds.

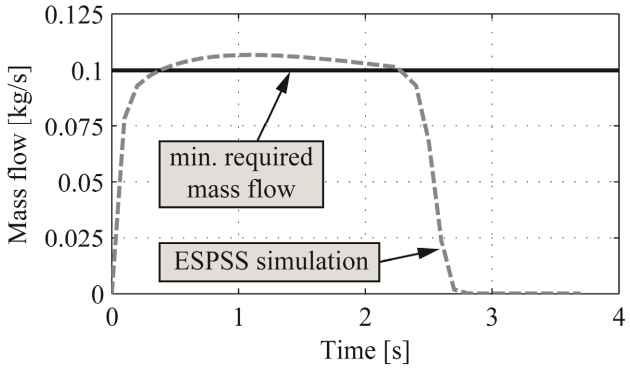

Fig. 19: **Mass flow through one Laval nozzle with the CASS**

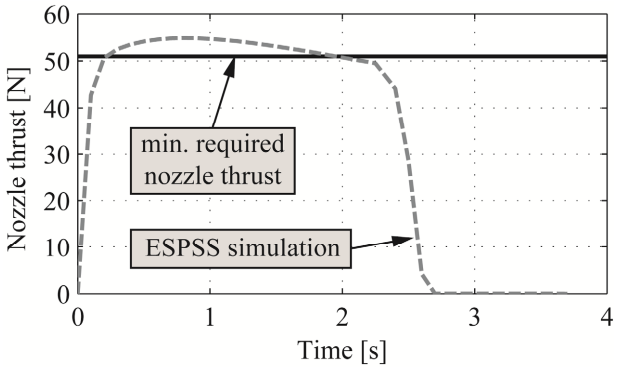

Fig. 20: **Thrust of one nozzle with the CAS**

The SASS uses shop air with a nearly constant pressure level for pressurized air supply. However, since the mass flow of the CASS decreases due to pressure tank emptying, the total pressure short before the Laval nozzles is also decreasing as Fig. 21 shows. The dotted line shows the CASS total pressure trend. It reaches almost the shop air total pressure level. However, the total pressure of the SASS in the supply pipes is lower since there are several pressure losses for instance due to friction. Nevertheless, the curve shows, that the total pressure level at the nozzle entry can be kept almost constant for the QSS operation time.

Besides the performance another requirement is the used installation space at the airframe. Since each nozzle has its own pressure tank of 9 l volume, in total 5 pressure tanks have to be integrated. The material of the tanks is of composite material and each tank weighs 5 kg. A possible solution shows Fig. 22. Here, 4 pressure tanks are integrated into the tail boom mounting cone of the BO 105. The fifth pressure tank is located between the main transmission and the firewall. Since the helicopter has two engines installed and each engine has a QSS, the pipes from the pressure tanks to the nozzles require a T-piece at the pressure tank joint. Therewith, a supply of each QSS can be guaranteed.

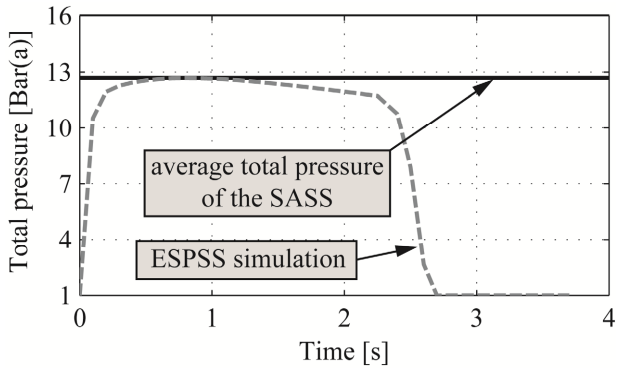

Fig. 21: **Total pressure short before the Laval nozzles with the CASS**

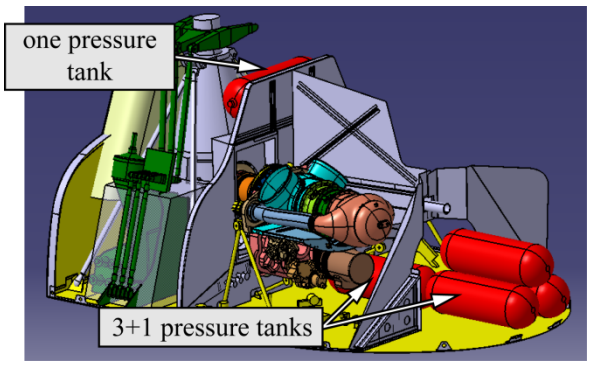

Fig. 22: **Arrangement of the 5 pressure tanks at the helicopter airframe**

However, a first estimation of the additional mass of the QSS with CASS leads to 80.55 kg. Considering 20% additional mass for system component mounting the total system mass is 96.65 kg. Hence, there are several options regarding handling this mass. One may be a reduction of the payload mass and therewith having no influence on helicopter flight performance. Another option is increasing the MTOW by the additional QSS mass which has a non-negligible influence on helicopter flight performance.

CONCLUSION AND OUTLOOK

This paper describes on the one hand the validation of the simulation program ESPSS for simulating the pressurized air supply of a QSS for turboshaft engines. On the other hand after validation a preliminary design of a compact pressurized air supply is defined, modelled and simulated. Therefore, several requirements are given which have to be fulfilled in the best manner. As a result of the validation the ESPSS tool delivers good results for parameters like pressure, temperature or mass flow. However, the measurement of the total air temperature inside the manifold of the QSS was insufficient. Improvements have to be done for better test data results. Finally, the program ESPSS was successfully evaluated for further design of a CASS. The design described in this paper revealed optimization potential. The required pressurized air volume is 45 liter in total for the pressure tanks. It should be reduced for better airframe integration. Furthermore, the air pressure in the tanks should be better used since at QSS deactivation the pressure tank has still approximately 200 Bar(a) air pressure. One approach may be a higher nozzle entry pressure resulting in a higher mass flow as well as a higher thrust. But it has to be further investigated whether the engine can sustain this new forces and moments. A critical part may be the bearings. Then, the requirement of a quasi-static total pressure of 12.3 Bar(a) at the nozzle entry may be reduced to a requirement of pressures between 15 Bar(a) and 9 Bar(a). An option is also a redesign of the Laval nozzles to meet new requirements which can be defined after the experience with the actual QSS configuration.

Furthermore the simulation does not respect the inertia and acceleration of the compressor and the increasing compressor end pressure. Simulating these effects would increase the simulation fidelity and may lead to better results for further final CASS design. With the realization of the final CASS design and integration at the test bed, further test data can be gained for validation of this simulation model. Other issues which have to be clarified are the effects coming along with a pyrotechnical valve. Since it has not been tested, there is not any evidence yet that the quite fast opening time of the valve may lead to serious flow issues inside the QSS.

REFERENCES

J. Hönle, A. Barth, W. Erhard, H.-P. Kau. *Engine Quick Start in Case of Emergency - A Requirement for Saving Fuel by Means of Engine Shutdown.* In Proceedings of the 38th European Rotorcraft Forum, Amsterdam, NL, September 2012

M. D. Paramour, M. J. Sapsard. *Future Technology and Requirements For Helicopter Engines*. AGARD Conference Proceedings No.302, Toulouse, France, May 1981

J. Hönle. *Ökonomische Optimierung von Triebwerksbetriebsstrategien von zweimotorigen Hubschraubern.* Ph.D. Thesis, TU München, 2014

L. Hull, H. Santo. *Development of a Rapid-Start System for the Boeing Model 502-2E Gas Turbine Engine*. SAE 670961, SAE Technical Paper, 1967

R. Gabler. *Betriebsverhalten von Wellenleistungsturbinen bei Verdichterinstabilitäten und Methoden zur Restabilisierung*. Ph.D. Thesis, TU München, 1998

M. Kerler, J. Hönle, W. Erhard, H.-P. Kau. *Helicopter Engine-in-the-Loop Test Setup.* In Proceedings of the 39th European Rotorcraft Forum, Moscow, Russia, September 2013

A. Isselhorst. *HM7B Simulation with ESPSS Tool on Ariane 5 ESC-A Upper Stage*. 46th *AIAA*/ASME/SAE/ASEE Joint Propulsion Conference & Exhibit, Nashville, TN, USA, July 2010

W. Ullrich. *CFD-Simulation einer Laval-Düse bei Überexpansion*. Unpublished study thesis, Institute for Flight Propulsion, TU München, 2011

A. Barth. *Konstruktion einer Verdichterpralldüse für das Triebwerk Allison 250-C20B.* Unpublished study thesis, Institute for Flight Propulsion, TU München, 2011

S. Maier. *Bauraumanalyse in der Engine Bay des Airbus Helicopters BO 105*. Unpublished study thesis, Institute for Flight Propulsion, TU München, 2014

R. Pérez-Vara, S. Mannu, O. Pin, R. Müller. *Overview of European Applications of EcosimPro to ECLSS, CELSS and ATCS*. 33rd International Conference on Environmental Systems (ICES), Vancouver, BC, Canada, July 2003. SAE Technical Paper 2003-01-2439

J. Moral, F. Rodríguez, J. Vilá, F. Di Matteo , J. Steelant. *1-D Simulation of Solid and Hybrid Combustors with EcosimPro/ESPSS*. Space Propulsion 2010

ESPSS. *European Space Propulsion System Simulation - EcosimPro Libraries User Manual*. ESA document 4000103800/11/NL/CP -TN4130. March, 2014